JCTC Journal of Chemical Theory and Computation

Structural, Energetic, and Infrared Spectra Insights into Methanol Clusters $(CH_3OH)_n$, for $n = 2-12$, 16, 20. ONIOM as an Efficient Method of Modeling Large Methanol Clusters

Marcos M. Pires and Vincent F. DeTuri*

Department of Chemistry, Ithaca College, Ithaca, New York 14850

Received November 29, 2006

Abstract: An investigation of gas-phase methanol clusters $(CH_3OH)_n$, where $n = 2-12$, 16, and 20, was completed with a range of computational methods: PM3, Hartree−Fock, B3LYP, MP2, and their combination using an ONIOM (our own *n*-layered integrated molecular orbital and molecular mechanics) method. Geometries, binding energies, and vibrational frequencies are reported. For all ab initio optimized structures, the cyclic isomer was found to be the most stable structure of all isomers investigated. The scaled OH frequency shift for $n = 1-4$ is found to be in good agreement with experimentally measured shifts. An ONIOM method, with the methyl group calculated at the low level and the hydroxyl group at the high level, proved to be an excellent way of reducing computational expense. The calculated enthalpies, geometries, and infrared spectra using an ONIOM method were comparable to that of a high-level calculation. Clusters were solvated using the integral equation formalism for the polarized continuum model method to compare with the microsolvation studies.

Introduction

The study of hydrogen-bonded clusters has been the subject of intense interest in the past decade, with water and methanol molecules receiving the greatest amount of attention.[1] Water is the most thoroughly investigated hydrogen-bonded cluster but is quite different from methanol. Water can form up to four hydrogen bonds, two as proton acceptors (via the lone-pair electrons on oxygen) and two as proton donors. Methanol generally only forms three strong hydrogen bonds, two as proton acceptors (via the lone-pair electrons on oxygen) and one as a proton donor. The methyl CH bonds may form weak hydrogen-bonding interactions. The bulky methyl group and the dipole it produces give methanol a more complex and asymmetrical cluster compared with water. This study aims to understand microscopic properties of methanol and relate those to the macroscopic properties. Specifically, we set out to determine the number of methanol molecules necessary to mimic the enthalpy of vaporization and geometric properties of bulk methanol. However, modeling a limited cluster size without molecular dynamics (MD) does not represent bulk methanol.

Much of the stabilization of methanol clusters comes from the very sensitive electronic interaction of the hydrogen bond. Thus, hydrogen-bonding fluids are described by the strength and number of hydrogen bonds formed. In water clusters of $n = 5-19$, the bonding energy calculated per hydrogen bond reproduces the binding energy of ice at 0 K better than the bonding energy calculated per water.[2] The dangling hydrogen bonds in the cluster contribute little to the energy stabilization of water. In methanol clusters, each molecule can donate only one hydrogen bond, a difference from water that has many structural and electronic consequences. An intriguing feature of hydrogen-bonded networks is that the acceptance of one hydrogen bond actually promotes the donation of an additional hydrogen bond in a process known as cooperativity or nonadditivity. The cooperativity effects have been previously calculated by ab initio methods for methanol clusters $(CH_3OH)_n$ for $n = 2-6$ isolated in a vacuum at the HF/aug-cc-pVDZ//HF/6-31G(d,p) level.[3] While, hydrophobic forces are also known to be part of the interaction within a methanol

* Corresponding author e-mail: vdeturi@ithaca.edu.

10.1021/ct600348x CCC: $37.00
Published on Web 03/27/2007

network, it is generally believed that the number of hydrogen bonds is what dominates the intermolecular interactions in hydrogen-bonded clusters.[3]

Density functional calculations, B3LYP/6-31+G(d), have been previously carried out on methanol clusters $(CH_3OH)_n$ for $n = 2-6$ isolated in a vacuum[4] and also at the B3LYP/6-31G(d) level for $n = 2-12$ in a vacuum.[5] Computational results indicate that the cyclic methanol clusters are the global minima when compared with chain, branched-cyclic, and branched-chain arrangements.[4,5] Cyclic structures maximize the number of hydrogen bonds and display an increase in cooperativity, thus yielding more favorable interactions among the members of the cluster.

Until recently, previous research on methanol clusters had been limited to single-digit numbers of molecules, and the few studies that examine higher levels, $(CH_3OH)_n$ for $n = 6-9$, were limited to minimal ab initio methods or less accurate methods.[1,6] A recent study investigated methanol clusters for $n = 2-12$ at the B3LYP/6-311+G(d,p)//B3LYP/6-31G(d) level.[5] It does not appear that methanol clusters have been studied computationally for cluster sizes greater than 12 molecules using an ab initio method. MD and Monte Carlo (MC) methods have been employed on much larger clusters (up to 256 methanol molecules);[7] however, they are limited by parametrization designed for small methanol clusters. It is not practical to account for 256 methanol molecules by an ab initio method, but an understanding of $n = 2-12$, 16, and 20 methanol clusters at a high-level ab initio method will improve the parameter set.

Herein, we also report the application of the ONIOM (our own *n*-layered integrated molecular orbital and molecular mechanics)[8] method to hydrogen-bonded methanol clusters. The ONIOM method has emerged as an efficient method to study hydrogen-bonding systems and microsolvation approximations.[9−11] A major advantage of the ONIOM method is its versatility. It comes in many flavors, thus making it possible to specify the appropriate method and level of theory of choice for individual atoms. In our study of methanol clusters, we use the integrated molecular orbital and molecular orbital method. The technique of applying a molecular orbital treatment to both layers has been successfully tested for non-methanol systems.[10] This means that both the high-level layer and the low-level layer will receive molecular orbital treatments.

There are many implications in the research of gas-phase methanol clusters that go beyond just the elucidation of how these macromolecular structures behave. Methanol molecules in large clusters are expected to have properties that are more similar to methanol in the condensed phase than to single methanol molecules. In particular, studies relating to methanol clusters may facilitate the modeling of complexation of solutes in methanol since it is well-known that the first solvation shell is particularly crucial in this respect. Solvation of organic acids by methanol has already been studied and so has proton transfer in methanol.[12−14] The principal goal of this work is to characterize the geometric, energetic, and vibrational features of methanol clusters by successively increasing the cluster size up to 20 molecules. Initially, we set out to identify the lowest-energy isomers for $(CH_3OH)_n$ where $n = 1-10$. The number of local minima of larger systems makes it difficult to thoroughly sample all of the different conformers for each size of methanol clusters at a high level of ab initio theory. However, we believe it is not necessary to find every minimum for a specific methanol cluster size. As we study them from the smaller cluster sizes to the larger ones, we should observe a pattern that will be mimicked with each additional methanol. Such patterns are not uncommon for hydrogen-bonded cluster networks. As Maheshwary et al. discovered with water clusters,[15] $(H_2O)_n$ where $n = 4$, 8, 12, 16, and 20 are cuboids while $(H_2O)_{10}$ and $(H_2O)_{15}$ are fused pentameric structures. Moreover, structures that contained one water molecule more than the cuboid series such as $n = 9$, 13, and 17 were very similar in structure to their cuboid correspondents.

Not all previously reported structures of extensively sized methanol clusters are in agreement.[1] It has been suggested that, for methanol clusters up to $n = 17$, the clusters do not have a dominant structure.[7] In molecular beam electric deflection experiments, the dimer was the predominant structure observed for methanol.[7] While it is possible for clusters to be in flux, that is, constant restructuring of the cluster size, many experimental results indicate that methanol can have a predictable pattern.[16]

Computational Methods

All calculations were carried out using the Gaussian 98 suite of programs[17] or the Gaussian 03 suite of programs.[18]

A common impediment to ab initio computational research of methanol clusters is the computational time required to model large clusters greater than six methanol molecules. Our first approach was to model many different conformers of each sized cluster, where $n = 1-10$, using the semiempirical method PM3. Geometry-optimized structures from the PM3 calculations were used as a starting point for HF/6-31+G(d,p) calculations. The addition of a diffuse basis set seems appropriate for a system in which hydrogen bonds contribute to the overall geometry and stabilization energy. Several of the lowest-energy PM3 structures were geometry-optimized at the HF/6-31+G(d,p) level. Basis set superposition error was calculated using the counterpoise keyword in Gaussian 03W on the optimized structures.[19,20] Additional calculations were employed using the hybrid density functional methods B3LYP and MP2. A number of basis sets were also investigated, 6-31G(d), 6-31+G(d,p), and 6-311+G-(d,p).

An ONIOM method[21] serves as an appropriate method to reduce the computational time it takes to describe methanol clusters. ONIOM methods were initially compared to one-layered calculations to verify their efficiency. Our two-level layer scheme replaces the methyl group with a hydrogen link atom in the high-level layer. This translates into a major reduction of computational time since each methanol molecule contributes 18 elecrons in the real system and 10 in the high-level system. Frequency calculations were used to verify the minima in geometry optimizations and provide thermochemical corrections to calculate the enthalpy and Gibbs energy at 298 K.

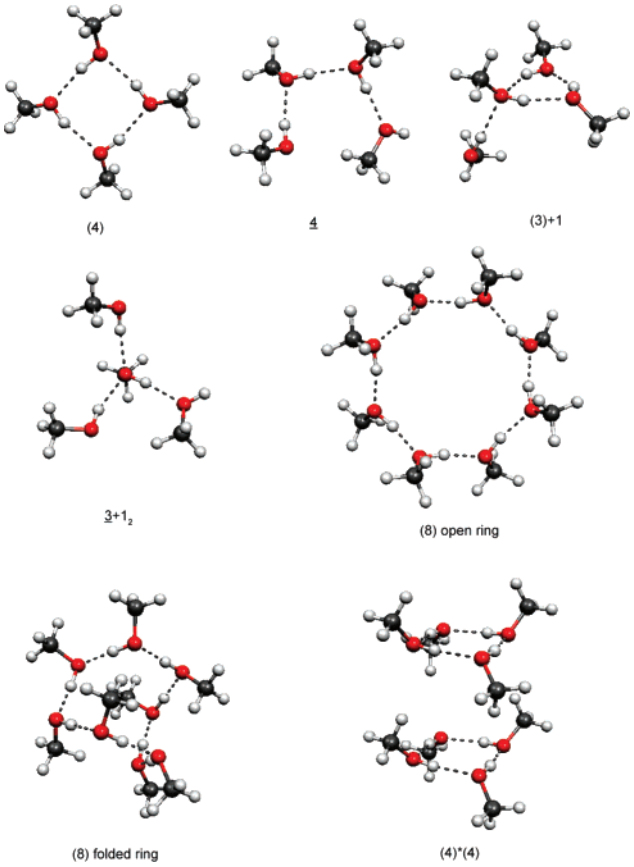

Figure 1. Representative geometries for several clusters using notation discussed in the text: ring tetramer (4), chain tetramer 4, cyclic trimer with attached methanol (3)+1, branched tetramer 3+1$_2$, (8) flat or open ring, (8) folded ring, and (4)*(4) stacked cluster.

To facilitate the representation of different combinations of same size structures, the following notations will be used: (X) represents a ring of size X; X represents a chain structure of size X; (X)+Y represents a ring of size X with an attached chain of size Y; (X)*(Y) represents a ring of size X stacked with a ring of size Y; and X+Y represents a chain of size X with a chain attached of size Y (sometimes the location of the attachment is also specified to make the representation clearer). Figure 1 diagrams several different methanol structures.

The average energy of a single methanol molecule in a $(MeOH)_n$ cluster can be calculated as $\bar{E}_n = E_n/n$. Comparing this energy to that of a single methanol in the gas phase, E_1, gave the per methanol stabilization energy calculated using eq 1.

$$\Delta\bar{E}_n = \frac{E_n}{n} - E_1 \qquad (1)$$

For a large cluster size, where n approaches Avogadro's number, the per methanol stabilization energy is equivalent to the enthalpy of solvation $\Delta\bar{E}_n = \Delta_{sol}H$ or MeOH(g) → MeOH(l). Equation 1 was used to compare the per methanol energy of n-sized clusters with the enthalpy of solvation. Inclusion of thermochemical values from a frequency analysis corrects the electronic energy to an enthalpy value and a Gibbs energy at 298 K.

The strength of a single hydrogen bond between methanol molecules is calculated by taking the difference in energy between the monomer and the dimer, $E_2 - E_1$. This difference in energy is compared to the increased energy found from one structure to the next structure after the addition of one methanol molecule. Hydrogen bond strength was estimated using eq 2.

$$E_{Hbond} = (E_n - E_{n-1}) - (E_2 - E_1) \qquad (2)$$

The energy stabilization from a single hydrogen bond is a measure of the energy difference between adding a hydrogen-bonding methanol molecule and an isolated methanol molecule. Some effects are not fully accounted for by using this method—mainly geometric rearrangements and dielectric forces.

Solvent effects using a dielectric medium were approximated using the integral equation formalism for the polarized continuum model (IEFPCM) method[22−24] on fully optimized clusters. The solvation energy was calculated by taking the difference between the gas-phase electronic energy and the solvent-wrapped electronic energy.

Results and Discussion

Cluster Geometry at the HF/6-31+G(d,p) Level. Semiempirical calculations were used to quickly scan a large range of isomers for each cluster size.

Conformers calculated using semiempirical methods that might be candidates as the most stable structure are tabulated in Table S1 in the Supporting Information. Initial geometries prior to optimization were constructed by guessing reasonable structures. Attempts at using a simulated annealing process or dynamics search were less effective and more costly at identifying unique cluster geometries.

Additional calculations were done at the HF/6-31+G(d,p) level for the $n = 2-7$ clusters on the three lowest-energy PM3 structures. The results from the HF/6-31+G(d,p) calculations are summarized in Table S2 of the Supporting Information. Basis set superposition errors are reported for each calculation and tabulated in Table S2 (Supporting Information). As the number of methanol molecules increases, the basis set superposition error also increases. In general, the ring structures show a greater correction than the branched or chain clusters due to the greater number of hydrogen-bonding interactions. The counterpoise correction for the cyclic structures as a function of cluster size gives a straight line with a slope of 3.2 ± 0.1 kJ/mol. Thus, the per methanol cluster energy should include a correction of 3 kJ/mol. This offset does not change the relative energy difference between the clusters; it only changes the absolute value compared with experimental results for the 6-31+G-(d,p) basis. The calculated dipole moments of the clusters are reported in Table S2 (Supporting Information) along with the geometric data of the OH bond, OO distance, and OHO angle. The addition of methanol molecules to clusters larger than six seems to have little or no effect on the bond lengths and bond angles of the hydrogen-bonding hydroxyl groups participating in hydrogen bonds. For the chain systems, the free OH bond length does not change significantly as the chain length increases. The per methanol energy for each

cluster geometry at the HF/6-31+G(d,p) level is summarized in Table S2 of the Supporting Information.

Three trimer conformers were studied at the HF/6-31+G-(d) level: a flat ring structure (3), a chain $\underline{3}$, and a single methanol molecule with two molecules attached to the two possible acceptor sites $\underline{2}+1$. The flat ring structure (3) had the lowest optimized energy at the HF/6-31+G(d,p) level of theory, consistent with previous studies.[25,26] The equilibrium geometry for the cyclic trimer is flat, resulting in poor overlap of the sp^3 orbitals compared to the noncyclic structures. However, the stabilization afforded by the additional hydrogen bonds compensates for the less favorable orbital overlap in the cyclic structure.

The cyclic tetramer arrangement with the methyl groups alternating between above and below the plane of the ring is the most stable of all arrangements. This configuration is in the S_4 point group. Other isomers were also considered, such as a cyclic tetramer with C_i symmetry and a (3)+1 isomer. As expected, both the C_i symmetry, and (3)+1 optimized structures were higher in energy than the S_4 tetramer.

The double acceptor−donor configuration serves as a branching point for an extended methanol cluster. The $\underline{3}+1_2$ isomer has been previously observed and characterized by Zwier and co-workers[4] and Boyd and Boyd.[5] The hydrogen bond donated by the branching methanol molecule is strengthened by accepting two hydrogen bonds from methanol molecules. However, the two hydrogen bonds to the branching molecule are weaker than a single hydrogen bond. Thus, the $\underline{3}+1_2$ structure is less stable than the cyclic (4) structure.

The pentamer isomers studied at the HF/6-31+G(d,p) level of theory were the (5), (4)+1, and (3)+1+1 structures. The ring structure has the lowest equilibrium energy of the three, being lower by 15.82 kJ/mol than the (4)+1 structure and 18.81 kJ/mol lower than the (3)+1+1 structure. The arrangement of alternating above−below methyl groups to the plane of the ring is mostly observed here, except for the necessary pairing of two methyl groups because of the odd number of molecules.

The four $(CH_3OH)_6$ structures studied at this level of theory were (6), (5)+1, (4)+1_1+1_2, and (4)+1_1+1_3. The ring structure is lower in energy by 12.40 kJ/mol, 25.66 kJ/mol, and 29.75 kJ/mol, respectively. It is evident from this set of data that there is a tendency for small methanol clusters to be in small rings. All four isomers had the same number of hydrogen bonds; thus, there must be a variable besides the absolute number of hydrogen bonds that leads to the stability of methanol structures. As discussed with the tetramer molecule, a branch point in the methanol cluster geometry could lead to an overall weakening of the total strength of the hydrogen bonds.

The ring octamer molecule (8) is lower in energy than the (4)*(4). In both structures, the methanol molecules are all single acceptors and single donors. The (8) and (4)*(4) structures are postulated to be very similar in energy if the two tetramers are able to find an arrangement in which they facilitate each other's stabilization. After several attempts to stack the two tetramers in different orientations with several different computational methods, the gas-phase octamer ring still is more stable than two stacked tetramer rings. It is possible that gas-phase structures simply do not have the proper dielectric assistance to force a geometric change in order for the two rings to conform around each other; however, this might be observed for liquid methanol.

At the HF/6-31+G(d,p) level, the lowest-energy structures for $n = 1-8$ are flat rings with the methyl groups being above, below, or approximately coplanar with the ring plane. The different cyclic structures vary by patterns of orientation of the methyl groups. Of the isomers investigated, the most stable structures are rings with an equal number of monomers above and below the plane. Other patterns such as above−above−below−below ($n = 4$) and above−below−in plane−above−below−in plane ($n = 6$) are slightly less stable. Rings with an odd number of monomers have no symmetry. As examples of such rings, the patterns of methyl group orientations are above−above−below ($n = 3$) and above−below−above−below−in plane ($n = 5$). Similar structures with different orientations of the methyl groups differ only by very small barriers of rotation.

All structures beyond the octamer at the HF/6-31+G(d,p) level of theory show a distinctive inclination toward a ring structure. However, beyond eight methanol molecules, there is no longer an "open" ring system; the ring system for $n = 9-12$ is "pinched". As the cluster of the methanol increases in size, it *may* begin to approximate liquid methanol. Bulk solvent effects have not been included in the optimization of the structures, and the expectation is that the clusters will attempt to minimize its volume. The "open" ring structure for $n > 8$ leads to an excluded volume; it is more favorable for clusters of $n > 8$ to form a "pinched" ring structure and fill the excluded volume with a dielectric.

At the HF/6-31+G(d,p) level of theory, the ring structures are found to be most stable for $n = 1-12$. The ring structure provides the maximum number of hydrogen bonds, when compared to chain and branched structures of the same size. Attempts to stack tetramers, both in an eclipsed nature and not, failed to produce meaningful results.

Table S2 (Supporting Information) tabulates the energy of clusters of size $n = 1-12$ calculated at the HF/6-31+G-(d,p) level. Comparison of the average energy per methanol calculated using eq 1 indicates that for the ring systems of $n \geq 6$ the average energy of a single methanol is about −30 kJ/mol. The average energy to convert from a cyclic structure to a chain cluster is about 27 kJ/mol with a greater energy needed to convert the larger conformers. The average energy of a methanol molecule in a chain is about 5 kJ/mol higher than the energy of a methanol molecule in a cyclic structure. This small energy difference indicates that there is only a slight preference for a single methanol to remain in a ring system over a chain system.

Single-point energy calculations at the B3LYP/6-311+G-(d,p) and MP2/6-311+G(d,p) levels were performed using the HF/6-31+G(d,p) optimized geometries. The B3LYP and MP2 results are tabulated in the Supporting Information, and the per methanol energy was calculated using eq 1. The higher-level energy calculations are consistent with the HF level of theory. Although the absolute energies are different,

Table 1. Geometry-Optimized Structures at the B3LYP Level Compared with Those at the HF Level

	HF/6-31+G(d,p)				B3LYP/6-31G(d)				B3LYP/6-311+G(d,p)			
cluster	dipole debye	$\bar{r}_{OH}$[a] Å	$\bar{r}_{OO}$[b] Å	$\bar{a}_{OHO}$[c] deg	dipole debye	$\bar{r}_{OH}$[a] Å	$\bar{r}_{OO}$[b] Å	$\bar{a}_{OHO}$[c] deg	dipole debye	$\bar{r}_{OH}$[a] Å	$\bar{r}_{OO}$[b] Å	$\bar{a}_{OHO}$[c] deg
$(MeOH)_1$	1.9729	0.942			1.6943	0.969			1.8894	0.961		
$(MeOH)_2$	3.2917	0.947	2.967	178.9	2.8777	0.977	2.810	159.7	3.1518	0.970	2.873	176.2
$(MeOH)_3$	2.7089	0.949	2.887	148.9	1.0560	0.986	2.745	152.3	0.8355	0.976	2.772	149.8
$(MeOH)_4$	0.0166	0.952	2.863	166.8	0.0005	0.994	2.703	168.7	0.0036	0.983	2.725	167.0
$(MeOH)_5$	0.5184	0.953	2.846	174.3	0.8582	0.995	2.692	176.4	0.6905	0.985	2.712	175.5
$(MeOH)_6$	0.0007	0.953	2.832	176.2	0.0021	0.995	2.683	174.4	0.0007	0.986	2.705	178.9
$(MeOH)_7$	0.0915	0.953	2.828	175.5	2.4285	0.995	2.690	174.9				
$(MeOH)_8$[d]	0.0043	0.953	2.828	174.5	0.0450	0.993	2.677	169.9	0.0670	0.985	2.697	176.3
$(MeOH)_8$[e]					0.1030	0.995	2.699	176.7	0.1112	0.986	2.715	176.5
$(MeOH)_9$	0.3864	0.953	2.830	174.5	2.1366	0.994	2.686	173.1				
$(MeOH)_{10}$	1.3795	0.953	2.832	175.1	1.2243	0.994	2.695	173.3				
$(MeOH)_{11}$	1.7175	0.953	2.829	175.1	2.7031	0.994	2.687	173.2				
$(MeOH)_{12}$	1.3207	0.953	2.831	175.2	2.0521	0.994	2.695	174.1				

[a] Average O−H bond length for hydrogen-bonding hydroxyl groups. [b] Average O−O distance between hydrogen-bonding methanol molecules. [c] Average O−H−O angle between hydrogen-bonding methanol molecules. [d] Structure is a flat ring. [e] Structure is a folded ring.

the trends are identical. At around five methanol molecules, the energy per methanol levels out to a consistent value.

Cluster Geometry at the B3LYP Level. Calculations at the HF/6-31+G(d,p) level of theory indicate that cyclic methanol clusters are lower in energy than chain clusters for $n = 3-12$. When the HF/6-31+G(d,p) geometry-optimized structures were used as an initial geometry, cluster geometries were further optimized using the B3LYP/6-31G-(d) level of theory for $n = 1-12$ and using the B3LYP/6-311+G(d,p) level of theory for $n = 1-6$ and 8. The geometry optimizations using the B3LYP method are tabulated and compared with HF calculations in Table 1. At the levels of theory reported in Table 1, it was not practical to extend the system beyond $n = 12$. For the B3LYP/6-31G(d) geometry optimizations for $n = 7$, the structure started as a flat ring structure and proceeded to fold. For the $n = 8$ system, the flat ring structure local minimum is 21 kJ/mol higher in energy than that for a folded ring system. And for $n = 9$, the geometry optimization started as a flat ring structure and optimized to a folded ring structure as well. Optimized geometries for $n > 6$ all converged to a folded or puckered OH ring structure instead of a flat OH ring structure. Interestingly, at the B3LYP/6-311+G(d,p) level, the flat $n = 8$ structure is 7 kJ/mol lower in energy than the folded structure, which contradicts the findings from the B3LYP/6-31G(d) level of theory. The flat structure for $n = 8$ is also the lowest-energy structure at the HF/6-31+G(d,p) level of theory. The folded and flat $n = 8$ structures are local true minima with no negative frequencies.

In general, the geometries optimized at the B3LYP level are consistent with that of the HF calculations. For $n \geq 4$, the average OH and OO distances converge to a constant value as the number of methanol molecules increases. For the $n = 4$ geometry, there is some ring strain for the OHO angle, but for the $n > 4$ geometries, the average OHO angle is consistent as the number of methanol molecules increases. The trends in the geometry optimization are generally insensitive to the level of theory except for the $n = 8$ cluster.

Our primary interest in this study is to identify an ab initio method to quickly and accurately model large methanol systems, specifically those governed by hydrogen bonding. The electronic energy is compared between the MP2/6-311+G(d,p)//B3LYP/6-31G(d) level of theory for $n = 1-4$ and 8 and the B3LYP/6-311+G(d,p) level of theory for $n = 1-6$ and 8 to the B3LYP/6-31G(d) level of theory. The B3LYP/6-31G(d) level is an inexpensive level of theory, and yet it appears to do a reasonable job in modeling large clusters. We have found that the B3LYP/6-31G(d) level produces nearly identical geometries (within 1%) to the geometries yielded by the 6-311+G(d,p) extended basis set. Our selection of the B3LYP/6-31G(d) level as an adequate method for obtaining reasonable methanol cluster geometries is consistent with findings by Boyd and Boyd.[5] For the geometry optimization of the structures, B3LYP/6-31G(d) is the level of theory of choice, and a larger basis set can be used to improve the accuracy of the energy calculation.[5]

Small clusters of $n = 3-12$ prefer to form a ring system over a branched ring system or chain structure.[5] A cyclic geometry maximizes the number hydrogen bonds where each methanol donates one hydrogen bond and accepts one hydrogen bond and methyl groups can rotate to minimize steric effects. Branched structures with a methanol accepting two hydrogen bonds leads to a methanol that accepts no hydrogen bonds and is a less favorable overall geometry. As the systems increase in size, the rings begin to pucker and fold, thus minimizing an excluded volume in the middle of the cluster.

Cluster Frequencies. Analytical second derivatives are calculated at the B3LYP/6-31G(d), HF/6-31+G(d,p), and B3LYP/6-311+G(d,p) levels for $n = 1-6$ and 8. The relative difference between the gas-phase OH stretching frequency $\upsilon_{OH}(1)$ and the cluster of size n average OH stretching frequency $\bar{\upsilon}_{OH}(n)$ is calculated using eq 3.

$$\frac{\bar{\upsilon}_{OH}(n) - \upsilon_{OH}(1)}{\upsilon_{OH}(1)} \times 100 \qquad (3)$$

Mirroring the average bond length for clusters of size $n \geq 4$, the average difference between the OH stretching frequency of the cluster and a single methanol converge. The

Table 2. Summary of per Methanol Enthalpy at 298 K and Gibbs Energy at 298 K Reported in kJ/mol[a]

	B3LYP/6-31G(d)				HF/6-31+G(d,p)						B3LYP/6-311+G(d,p)	
	B3LYP/6-31G(d)		MP2/6-311+G(d,p)		HF/6-31+G(d,p)		B3LYP/6-311+G(d,p)		MP2/6-311+G(d,p)		B3LYP/6-311+G(d,p)	
cluster	ΔH_{298}	ΔG_{298}	ΔH_{298}	ΔG_{298}	ΔH_{298}	ΔG_{298}	ΔH_{298}	ΔG_{298}	ΔH_{298}	ΔG_{298}	ΔH_{298}	ΔG_{298}
$(MeOH)_2$	−12	4	−10	5	−7	7	−8	5	−10	4	−9	6
$(MeOH)_3$	−28	−2	−20	6	−16	10	−18	8	−22	5	−19	6
$(MeOH)_4$	−36	−6	−29	1	−19	8	−24	4	−28	0	−26	3
$(MeOH)_5$	−37	−6			−22	9	−26	4	−30	0	−28	4
$(MeOH)_6$	−38	−6			−22	8	−27	3	−31	−1	−29	3
$(MeOH)_8$					−22	8	−27	4	−31	−1		
$(MeOH)_8$[b]	−39	−3	−34	2							−28	7
MAD	1		7		17		13		8		10	

[a] The MAD (mean average deviation) compares the $n = 4$, 5, 6, and 8 clusters with the experimental value of $\Delta H_{298} = -38.4$ kJ/mol. [b] Folded ring geometry for $(MeOH)_8$.

relative difference using the B3LYP method for the 6-311+G(d,p) basis and the 6-31G(d) basis is about 12%, and the average HF/631+G(d,p) difference is about 5%. When the B3LYP method is used, there is very little difference between the 6-311+G(d,p) basis and the 6-31G(d) basis. The absolute difference in the gas-phase OH stretching frequency using the B3LYP method is 94 cm^{-1} or 2%. Vibrational frequencies at each level of theory for clusters $n = 1-6$ and 8 can be found in the Supporting Information. To evaluate the quality of the frequency calculations, the calculated IR-active OH stretching modes are compared with known experimental values.[25,27,28] The calculated stretching frequencies are scaled by the appropriate scaling factors of 0.9173 for the HF/6-31+G(d,p) level of theory, 0.9806 for the B3LYP/6-31G(d) level of theory, and 0.98 for the B3LYP/6-311+G(d,p) level of theory. After scaling, the B3LYP/6-31G(d) level of theory has a mean average deviation (MAD) = 30 cm^{-1} and comes closest to reproducing the experimental OH stretching frequencies. The B3LYP/6-311+G(d,p) level of theory has a MAD = 65 cm^{-1} and is comparable to the B3LYP/6-31G(d) level of theory. The HF/6-31+G(d,p) level of theory has the largest mean absolute deviation of 308 cm^{-1} but is still within 10% of the experimental values.

The frequency comparison for each structure and the relative cluster energy indicate that the B3LYP/6-31G(d) level of theory is sufficiently accurate in modeling the neutral methanol cluster geometry.

Cluster Energetics. Thermochemical analysis from the analytical second derivatives provides a correction to calculate the enthalpy and Gibbs energy at 298 K. The per methanol enthalpy at 298 K is calculated using scaled vibrational energies.[29] These values are reported in Table 2 and compared with the experimental value[30] of -38.4 ± 0.3 kJ/mol. It is evident from the tabulation that, of all the methods used in this study, the B3LYP/6-31G(d) level of theory yields values that are most similar to the experimental values. Also, only the B3LYP/6-31G(d) level of theory gave a negative Gibbs energy at 298 K (Table 2) for the $n = 3-8$ clusters. A negative Gibbs energy implies a favorable structure. The most stable clusters are the $n = 4-6$ at the B3LYP/6-31G(d) level of theory when the entropy of complexation is considered. The $n = 4-6$ and 8 clusters at the MP2/6-311+G(d,p)//HF/6-31+G(d,p) level have a Gibbs energy of 0 or −1 kJ/mol. Other levels of theory investigated generated positive Gibbs energies, implying that the clusters are not stable. It is possible that there are deficiencies in the entropy calculation from vibrational frequencies.

ONIOM Calculations. For clusters of five to six methanols, the average hydrogen-bond lengths and average solvation energies approach an asymptotic value. To accurately represent a large methanol system including a hydrogen-bonding network and dielectric effects, the cluster should consist of more than six methanol molecules. Accurate geometries and energies for bulky systems must include hydrogen bonding; however, as the cluster size increases the computational resources become costly. The methyl group of methanol does not directly participate in hydrogen-bonding interactions but is significant in aligning the dipole of methanol and contributes to the dielectric strength of the system. To accurately and efficiently model a large methanol system beyond $n = 12$, we use a two-level ONIOM method. The real $(CH_3OH)_n$ system is modeled at a computationally inexpensive level of theory, and the hydrogen-bonding network $(OH)_n$ system is modeled at a high level of theory, with hydrogen as a link atom in the high layer.

Geometry optimizations were performed on the cyclic methanol tetramer (4) and compared to one-layer calculations. In order to find the optimum set of low and high level of theory for the two-layered method, multiple combinations of two-level ONIOM calculations were tried on the methanol tetramer. The values for OH length, OO length, and OHO angle are tabulated in Table 3. The values are sorted by their deviations from the B3LYP/6-31G(d) level of theory. The cheapest method within a 2% accuracy to the B3LYP/6-31G(d) level of theory is the B3LYP/6-31G(d):PM3 level of theory. Treating the methyl groups with the AM1 level gives comparable results. We found that using HF/STO-3G on the low layer yields the most accurate values, but a HF/STO-3G calculation is not significantly cheaper than a full B3LYP/6-31G(d) calculation.

With the optimized ONIOM conditions in hand, we proceeded to apply the B3LYP/6-31G(d):PM3 level of theory to methanol clusters $n = 1-12$, 16, and 20. The geometric results and the per methanol single-point electronic energies are shown in Table 4. The ONIOM calculations reduced the computational time by a factor of 6 compared with calculations at the B3LYP/6-31G(d) level. For example, a single optimization step for the $n = 5$ cluster on a 32-bit Intel

Table 3. Geometry Comparisons of Cyclic Methanol Tetramer[a]

method	$\bar{r}_{OH}$	$\bar{r}_{OO}$	$\bar{a}_{OHO}$	$\delta(\bar{r}_{OH})$	$\delta(\bar{r}_{OO})$	$\delta(\bar{a}_{OHO})$
B3LYP/6-31G(d)	0.994	2.703	168.7	0.0%	0.0%	0.0%
B3LYP/6-31G(d):HF/STO-3G	0.994	2.703	168.7	0.0%	0.0%	0.0%
B3LYP/6-31+G(d)	0.989	2.714	167.8	−0.5%	0.4%	−0.5%
B3LYP/6-31+G(d,p):HF/STO-3G	0.989	2.716	167.8	−0.5%	0.5%	−0.6%
B3LYP/6-31G(d):AM1	0.999	2.733	168.6	0.5%	1.1%	0.0%
B3LYP/6-31G(d):PM3	0.991	2.754	168.7	−0.3%	1.9%	0.0%
B3LYP/6-31+G(d):HF/6-31G(d)	0.986	2.722	167.1	−0.8%	0.7%	−0.9%
B3LYP/6-311+G(d,p)	0.983	2.725	167.0	−1.1%	0.8%	−1.0%
MP2/6-31G(d):AM1	0.993	2.780	168.2	−0.1%	2.8%	−0.3%
MP2/6-31G(d):PM3	0.986	2.798	168.2	−0.8%	3.5%	−0.3%
B3LYP/6-311+G(d):AM1	0.986	2.762	164.2	−0.8%	2.2%	−2.7%
B3LYP/6-31+G(d,p):PM3	0.984	2.774	165.0	−1.0%	2.6%	−2.2%
MP2/6-31+G(d,p):HF/STO-3G	0.984	2.787	164.6	−1.0%	3.1%	−2.5%
B3LYP/6-311+G(d,p):PM3	0.978	2.795	164.4	−1.6%	3.4%	−2.6%
PM3	0.964	2.731	162.6	−3.1%	1.0%	−3.6%
MP2/6-311+G(d,p):PM3	0.971	2.809	163.6	−2.3%	3.9%	−3.0%
HF/6-31G(d,p)	0.953	2.830	166.9	−4.1%	4.7%	−1.1%
HF/6-31+G(d,p)	0.952	2.863	166.8	−4.2%	5.9%	−1.2%
HF/6-31+G(d):HF/STO-3G	0.958	2.891	163.9	−3.7%	7.0%	−2.8%
HF/6-31+G(d,p):PM3	0.951	2.919	163.7	−4.4%	8.0%	−3.0%

[a] Average O−O bond distance, average O−H bond distance, and average O−H−O angle. Distances are reported in angstroms, and angles are reported in degrees. The deviation from the B3LYP/6-31G(d) optimization is reported.

Table 4. Geometry-Optimized Structures at the ONIOM B3LYP/6-31G(d):PM3 Level

cluster	dipole debye	OH[a] Å	OO[b] Å	OHO[c] deg	$\Delta\bar{E}_n$[d]	ΔH_{298}[e]	ΔG_{298}[f]
$(MeOH)_1$	1.5477	0.965					
$(MeOH)_2$	1.4228	0.974	2.911	163.1	−14	−11	4
$(MeOH)_3$	1.0858	0.984	2.799	153.0	−32	−27	0
$(MeOH)_4$	0.0006	0.991	2.754	168.7	−40	−35	−3
$(MeOH)_5$	1.4581	0.991	2.752	174.5	−41	−36	−2
$(MeOH)_6$	0.0286	0.990	2.752	176.7	−41	−36	0
$(MeOH)_7$	0.6323	0.991	2.754	177.2	−42	−37	−1
$(MeOH)_8$	0.1997	0.991	2.755	176.1	−43	−37	1
$(MeOH)_9$	4.1048	0.991	2.750	176.2	−44	−39	1
$(MeOH)_{10}$	1.4764	0.990	2.754	174.3	−43	−37	1
$(MeOH)_{11}$	2.2169	0.991	2.753	175.7	−42	−37	2
$(MeOH)_{12}$	2.0048	0.991	2.750	176.7	−44	−38	1
$(MeOH)_{16}$	5.2732	0.991	2.753	173.6	−44	−38	3
$(MeOH)_{20}$[g]	3.7549	0.991	2.757	173.9	−45	−38	4

[a] Average O−H bond length for hydrogen-bonding hydroxyl groups. [b] Average O−O distance between hydrogen-bonding methanol molecules. [c] Average O−H−O angle between hydrogen-bonding methanol molecules. [d] Per methanol electronic energy. [e] Per methanol enthalpy at 298 K. [f] Per methanol Gibbs energy at 298 K. [g] The geometry is (19)+1; see text for details.

processor running Windows using the ONIOM method required approximately 6 min, whereas the B3LYP/6-31G(d) level required approximately 35 min to process the same optimization. On average, the ONIOM method did not require more optimization steps to find a minimum. Figure 2 diagrams the geometry-optimized structures from the ONIOM calculations. Results from the B3LYP/6-31G(d) calculations are also tabulated in Table 4. At most, the ONIOM calculated enthalpy at 298 K is 3 kJ/mol different than the B3LYP/6-31G(d) calculations for $n = 1-6$ and 8. Thus, B3LYP/6-31G(d):PM3 is a suitable model for calculating small- and intermediate-sized methanol clusters. The two-level ONIOM was applied to even larger clusters, expanding this study up to $n = 20$ by investigating $n = 1-12$, 16, and 20. The relative energetic and geometric parameters converge after about $n = 6$ and extend out to $n = 20$; therefore, the clusters $n = 13-15$ and $17-19$ were not examined. The $(CH_3OH)_{20}$ cluster was optimized several times, and the lowest-energy cluster was a (19)+1 branched ring. Several attempts were made to retain a (20) ring system but were unsuccessful. This indicates that there may be an upper limit to the size of a ring system. The open-ring systems are no longer favorable for $n > 6$, and around $n = 20$, branched folded ring systems appear to be more favorable than cyclic systems.

The strength of a single hydrogen bond is estimated for each cluster using eq 2. Table 5 tabulates the results from additional hydrogen bonds at the B3LYP/6-31G(d) level of theory and using the B3LYP/6-31G(d):PM3 ONIOM method. Stabilization by a single hydrogen bond in methanol clusters reaches a maximum at $n = 3$.

Table 6 summarizes the single-point energies using the IEFPCM model on the B3LYP/6-31G(d) optimized structures. The average solvation energy is −21 kJ/mol, which does not correlate well with the experimental value of −38.4 kJ/mol. The solvation energy also varies depending on the size of the methanol cluster. For example, clusters of $n = 2$ have the greatest solvation energy of −34 kJ/mol, while the $n = 3$ cluster has a solvation energy of −13 kJ/mol.

Conclusion

We tested several different levels of theory in finding single-point energies for large methanol clusters. The general trend of the energy per methanol molecule for all methods is very similar; after approximately four or five methanol molecules, the energy per methanol leveled off and started to approach an asymptotical value. Several ab initio and ONIOM methods

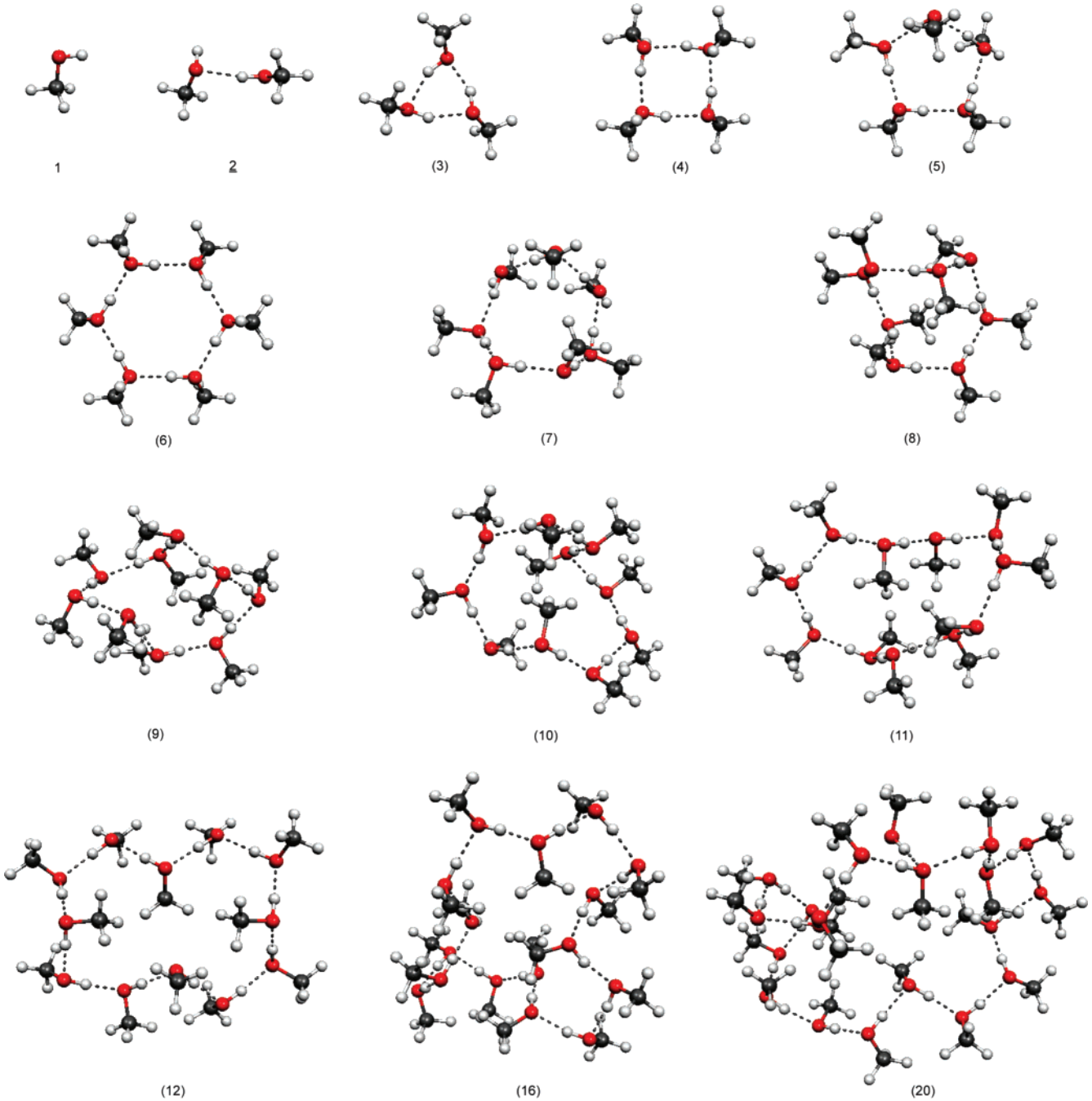

Figure 2. Geometry-optimized structures at the ONIOM (B3LYP/6-31G(d):PM3) level.

are applied to the system. When the results for the ONIOM method are compared to that of nonlayered calculations, it becomes evident that the considerably faster ONIOM method models the cluster to complete satisfaction. Geometric, energetic, and vibrational data support this conclusion. The advantage of the ONIOM method is that it provides the accuracy of a high-level calculation for the hydrogen-bonding network of methanol but requires the computation resources of a much smaller system. The geometry of methanol clusters is established for one-layer systems using density functional theory methods and a basis set, including diffuse and polarization functions. The ONIOM calculations are able to efficiently and accurately reproduce the geometry of the methanol clusters. The frequency analysis provided thermochemical corrections to calculate enthalpy and Gibbs energy at 298 K to compare with the experimental enthalpy of solvation and Gibbs energy of solvation. Our implementation of the ONIOM method reduces the size of the high-level calculation from an 18-electron system to a 10-electron system. A major advantage to this reduction is that one is able to double the size of the system using the same computational resources. A modification to the ONIOM method that treats all two-body interactions with a high-level QM method and the many-body interactions with a low-level QM should allow greater reduction in the cost of accurate calculations of methanol clusters.[31]

For methanol clusters with $n \leq 6$, the geometries optimize to an open-ring structure. Large methanol clusters $n > 6$ optimized to a folded ring or pinched ring structure. Comparisons between single-ring structures, branched struc-

Table 5. Hydrogen-Bond Stabilization Effects Calculated Using eq 2 Comparing Electronic Energy at the B3LYP/6-31G(d) and B3LYP/6-31G(d):PM3 Levels Using the ONIOM Method

cluster	B3LYP/6-31G(d)	B3LYP/6-31G(d):PM3
$(MeOH)_3$	−40	−39
$(MeOH)_4$	−35	−33
$(MeOH)_5$	−17	−16
$(MeOH)_6$	−16	−11
$(MeOH)_7$	−17	−24
$(MeOH)_8$	−25	−19
$(MeOH)_9$	−1	−20
$(MeOH)_{10}$	−19	−5
$(MeOH)_{11}$	−11	−11
$(MeOH)_{12}$	−23	−27

[a] Energies are reported in kJ/mol.

Table 6. Single-Point Solvation Energy and Optimized Geometry Energy at the B3LYP/6-31G(d) Level Using the IEFPCM Method[a]

cluster	E_{solv}	per MeOH	cluster	E_{solv}	per MeOH
$(MeOH)_1$	−22		$(MeOH)_5$	−16	−24
$(MeOH)_2$	−34	−10	$(MeOH)_6$	−15	−24
$(MeOH)_3$	−13	−16	$(MeOH)_7$	−18	−25
$(MeOH)_4$	−13	−23	$(MeOH)_8$	−19	−26

[a] Energies are reported in kJ/mol.

tures, and multiple-ring structures indicate that single-ring systems are lower in energy. As the clusters become larger, the fluidity of the structure increases, and the global minimum at 0 K may be a pinched ring system. However, at thermal energies, a large cluster may readily sample branched structures and multiple-ring structures. Methanol clusters receive the most stabilization from hydrogen bonds, and the ring structures maximize the number of hydrogen bonds, resulting in optimized OHO angles, OO distances, and OH distances. In a ring system, one methanol molecule will act as both a donor and acceptor of a hydrogen bond. Ring structures provide the most spacing between the bulky methyl groups, further elevating the preference for rings over a branched or chain system for a static geometry.

Small clusters consisting of up to six methanol molecules do not necessarily represent bulk properties. However, our results indicate that cluster properties begin to reach an asymptotic limit after six methanol molecules are calculated in a cluster.

Acknowledgment. We thank the Camille & Henry Dreyfus Foundation and Ithaca College for funding. Ryan Adler, Jonathan Hershenson, Brian Hoyt, and Erica Schlesinger aided in the preliminary and final calculations on dielectric wrapping.

Supporting Information Available: Table S1 tabulates several of the PM3 calculations of the clusters. Tables S2 and S3 tabulate the HF/6-31+G(d,p) geometries and electronic energies in hartrees. Table S4 compares the single-point electronic energies in hartrees at the HF/6-31+G(d,p) geometry for a B3LYP/6-311+G(d,p) and MP2/6-311+G(d,p) energy calculation. Table S5 compares the electronic energies in hartrees at several levels of theory. Table S6 tabulates calculated unscaled vibrational frequencies. Cartesian coordinates for all clusters at the HF/6-31+G(d,p), B3LYP/6-31G(d), B3LYP/6-311+G(d,p), ONIOM(B3LYP/6-31G(d):PM3), and IEFPCM B3LYP/6-31G(d) levels are reported. Frequencies for all ONIOM cluster geometries are also reported. This material is available free of charge via the Internet at http://pubs.acs.org.

References

(1) Buck, U.; Huisken, F. *Chem. Rev.* **2000**, *100*, 3863−3890.

(2) Su, J. T.; Xu, X.; Goddard, W. A., III *J. Phys. Chem. A* **2004**, *108*, 10518−10526.

(3) Sum, A. K.; Sandler, S. I. *J. Phys. Chem. A* **2000**, *104*, 1121−1129.

(4) Hagemeister, F. C.; Gruenloh, C. J.; Zwier, T. S. *J. Phys. Chem. A* **1998**, *102*, 82−94.

(5) Boyd, S. L.; Boyd, R. J. *J. Chem. Theory Comput.* **2007**, *3*, 54−61.

(6) Buck, U.; Siebers, J.; Wheatley, R. J. *J. Chem. Phys.* **1998**, *108*, 20−32.

(7) Wright, D.; El-Shall, M. S. *J. Chem. Phys.* **1996**, *105*, 11199−11208.

(8) Svensson, M.; Humbel, S. F. R. D. J.; Matsubara, T.; Sieber, S.; Morokuma, K. *J. Phys. Chem.* **1996**, *100*, 19357−19363.

(9) Re, S.; Morokuma, K. *J. Phys. Chem. A* **2001**, *105*, 7185−7197.

(10) Tschumper, G. S.; Morokuma, K. *THEOCHEM* **2002**, *592*, 137−147.

(11) Hopkins, B. W.; Tschumper, G. S. *Int. J. Quantum Chem.* **2004**, *96*, 294−302.

(12) Lin, X.; Zhao, C.; Phillips, D. L. *J. Org. Chem.* **2005**, *70*, 9279−9287.

(13) Koch, H. F.; Mishima, M.; Zuilhof, H. *Ber. Bunsen. Ges.* **1998**, *102*, 567−572.

(14) DeTuri, V. F.; Koch, H. F.; Koch, J. G.; Lodder, G.; Mishima, M.; Zuilhof, H.; Abrams, N. M.; Anders, C. E.; Biffinger, J.; Han, P.; Kurland, A. R.; Nichols, J. M.; Ruminski, A. M.; Smith, P. R.; Vasey, K. *J. Phys. Org. Chem.* **2006**, *19*, 308−317.

(15) Maheshwary, S.; Patel, N.; Sathyamurthy, N.; Kulkarni, A. D.; Gadre, S. R. *J. Phys. Chem. A* **2001**, *105*, 10525−10537.

(16) Tschumper, G. S.; Gonzales, J. M.; Schaefer, H. F., III *J. Chem. Phys.* **1999**, *111*, 3027−3034.

(17) Frisch, M. J.; Trucks, G. W.; Schlegel, H. B.; Gill, P. M. W.; Johnson, B. G.; Robb, M. A.; Cheeseman, J. R.; Keith, T.; Petersson, G. A.; Montgomery, J. A.; Raghavachari, K.; Al-Laham, M. A.; Zakrzewski, V. G.; Ortiz, J. V.; Foresman, J. B.; Cioslowski, J.; Stefanov, B. B.; Nanayakkara, A.; Challacombe, M.; Peng, C. Y.; Ayala, P. Y.; Chen, W.; Wong, M. W.; Andres, J. L.; Replogle, E. S.; Gomperts, R.; Martin, R. L.; Fox, D. J.; Binkley, J. S.; Defrees, D. J.; Baker, J.; Stewart, J. P.; Head-Gordon, M.; Gonzalez, C.; Pople, J. A. *Gaussian 98*; Gaussian, Inc.: Pittsburgh, PA, 1998.

(18) Frisch, M. J.; Trucks, G. W.; Schlegel, H. B.; Scuseria, G. E.; Robb, M. A.; Cheeseman, J. R.; Montgomery, J. J. A.; Vreven, T.; Kudin, K. N.; Burant, J. C.; Millam, J. M.; Iyengar, S. S.; Tomasi, J.; Barone, V.; Mennucci, B.; Cossi, M.; Scalmani, G.; Rega, N.; Petersson, G. A.; Nakatsuji, H.;

Hada, M.; Ehara, M.; Toyota, K.; Fukuda, R.; Hasegawa, J.; Ishida, M.; Nakajima, T.; Honda, Y.; Kitao, O.; Nakai, H.; Klene, M.; Li, X.; Knox, J. E.; Hratchian, H. P.; Cross, J. B.; Bakken, V.; Adamo, C.; Jaramillo, J.; Gomperts, R.; Stratmann, R. E.; Yazyev, O.; Austin, A. J.; Cammi, R.; Pomelli, C.; Ochterski, J. W.; Ayala, P. Y.; Morokuma, K.; Voth, G. A.; Salvador, P.; Dannenberg, J. J.; Zakrzewski, V. G.; Dapprich, S.; Daniels, A. D.; Strain, M. C.; Farkas, O.; Malick, D. K.; Rabuck, A. D.; Raghavachari, K.; Foresman, J. B.; Ortiz, J. V.; Cui, Q.; Baboul, A. G.; Clifford, S.; Cioslowski, J.; Stefanov, B. B.; Liu, G.; Liashenko, A.; Piskorz, P.; Komaromi, I.; Martin, R. L.; Fox, D. J.; Keith, T.; Al-Laham, M. A.; Peng, C. Y.; Nanayakkara, A.; Challacombe, M.; Gill, P. M. W.; Johnson, B.; Chen, W.; Wong, M. W.; Gonzalez, C.; Pople, J. A. *Gaussian 03*, revision C.02; Gaussian, Inc.: Wallingford, CT, 2004.

(19) Simon, S.; Duran, M.; Dannenber, J. J. *J. Chem. Phys.* **1996**, *105*, 11024−11031.

(20) Boys, S. F.; Bernardi, F. *Mol. Phys.* **1970**, *196*, 553−566.

(21) Maseras, F.; Morokuma, K. *J. Comput. Chem.* **1995**, *16*, 1170−1179.

(22) Cancès, M. T.; Mennucci, B.; Tomasi, J. *J. Chem. Phys.* **1997**, *107*, 3032−3041.

(23) Cossi, M.; Barone, V. M. B.; Tomassi, J. *Chem. Phys. Lett.* **1998**, *286*, 253−260.

(24) Mennucci, B.; Tomasi, J. *J. Chem. Phys.* **1997**, *106*, 5151−5158.

(25) Provencal, R.; Paul, J. B.; Roth, K.; Chapo, C.; Casaes, R. N.; Saykally, R. J.; Tschumper, G. S.; Schaefer, H. F., III *J. Chem. Phys.* **1999**, *110*, 4258−4267.

(26) Mó, O.; Yáñez, M.; Elguero, J. *J. Chem. Phys.* **1997**, *107*, 3592−3601.

(27) Fu, H. B.; Hu, Y. J.; Bernstein, E. R. *J. Chem. Phys.* **2006**, *124*, 024302.

(28) Shimanouchi, T. In *NIST Chemistry WebBook, NIST Standard Reference Database Number 69*; Linstrom, P. J., Mallard, W. G., Eds.; National Institute of Standards and Technology: Gaithersburg, MD, 2005.

(29) Scott, A. P.; Radom, L. *J. Phys. Chem.* **1996**, *100*, 16502−16513.

(30) Afeefy, H. Y.; Liebman, J. F.; Stein, S. E. In *NIST Chemistry WebBook, NIST Standard Reference Database Number 69*; Linstrom, P. J., Mallard, W. G., Eds.; National Institute of Standards and Technology: Gaithersburg, MD, 2005.

(31) Tschumper, G. S. *Chem. Phys. Lett.* **2006**, *427*, 185−191.

CT600348X